Meteoritics & Planetary Science 1–12 (2022)
doi: 10.1111/maps.13787

The manufacture and origin of the Tutankhamen meteoritic iron dagger

Takafumi MATSUI[1,2], Ryota MORIWAKI[2], Eissa ZIDAN[3], and Tomoko ARAI[1]*

[1]Planetary Exploration Research Center, Chiba Institute of Technology, 2-17-1, Tsudanuma, Narashino, Chiba 275-0016, Japan
[2]Institute for Geo-Cosmology, Chiba Institute of Technology, 2-17-1, Tsudanuma, Narashino, Chiba 275-0016, Japan
[3]Conservation Center, Grand Egyptian Museum, El Remayah Square, Cairo-Alex. Road, Pyramids, Giza Governorat, Egypt
*Corresponding author. E-mail: tomoko.arai@it-chiba.ac.jp

(Received 10 June 2021; revision accepted 22 December 2021)

Abstract–The Iron Age was the time when people acquired iron processing technology and is generally thought to have begun after 1200 B.C. Some prehistoric iron artifacts made of iron meteorites are dated from the Bronze Age. A nicely preserved meteoritic iron dagger was found in the tomb of King Tutankhamen (1361–1352 B.C.) of ancient Egypt. Yet, its manufacturing method and origin remain unclear. Here, we report nondestructive two-dimensional chemical analyses of the Tutankhamen iron dagger, conducted at the Egyptian Museum of Cairo. Elemental mapping of Ni on the dagger blade surface shows discontinuous banded arrangements in places with "cubic" symmetry and a bandwidth of about 1 mm, suggesting a Widmanstätten pattern. The intermediate Ni content (11.8 ± 0.5 wt%) with the presence of the Widmanstätten pattern implies the source meteorite of the dagger blade to be octahedrite. The randomly distributed sulfur-rich black spots are likely remnants of troilite (FeS) inclusions in iron meteorite. The preserved Widmanstätten pattern and remnant troilite inclusion show that the iron dagger was manufactured by low-temperature (<950 °C) forging. The gold hilt with a few percent of calcium lacking sulfur suggests the use of lime plaster instead of gypsum plaster as an adhesive material for decorations on the hilt. Since the use of lime plaster in Egypt started during the Ptolemaic period (305–30 B.C.), the Ca-bearing gold hilt hints at its foreign origin, possibly from Mitanni, Anatolia, as suggested by one of the Amarna letters saying that an iron dagger with gold hilt was gifted from the king of Mitanni to Amenhotep III, the grandfather of Tutankhamen.

INTRODUCTION

Some prehistoric iron artifacts made of iron meteorites are dated from the Bronze Age (e.g., Bjorkman, 1973; Comelli et al., 2016; Johnson et al., 2013; Nakai et al., 2008; Stevenson, 2009). The oldest iron dagger made of meteoritic iron was excavated at Alacuhöyük in Anatolia, Turkey (Nakai et al., 2008). Anatolia is the peninsula of land that presently constitutes the Asian part of Turkey. This dagger dates to the Early Bronze Age, ca. 2300 B.C., and it was found in a burial context. This early find suggests that the technology to work meteoritic iron to make complex objects is at least 4300 yr old and may have been known in Anatolia, where iron smelting was later developed. This dagger is so heavily corroded that it is difficult to study how it was manufactured. The Tutankhamen dagger blade, in contrast, is well preserved and thus provides a good opportunity for study.

Tutankhamen's iron dagger (Fig. 1a) made of meteoritic iron (Comelli et al., 2016) was found in his tomb (Carter & Mace, 1923–1927–1933). Tutankhamen reigned (1361–1352 B.C.) during Egypt's 18th dynasty—that is, during the Late Bronze Age, before the period of widespread iron use known as the Iron Age. The high quality of this iron object indicates that the skill to work meteoritic iron was well established at that time. Yet, its manufacturing method remains unclear (Comelli et al., 2016). A number of manufacturing processes are possible, such as cold working, in which an iron meteorite is cut and polished; hot working, involving

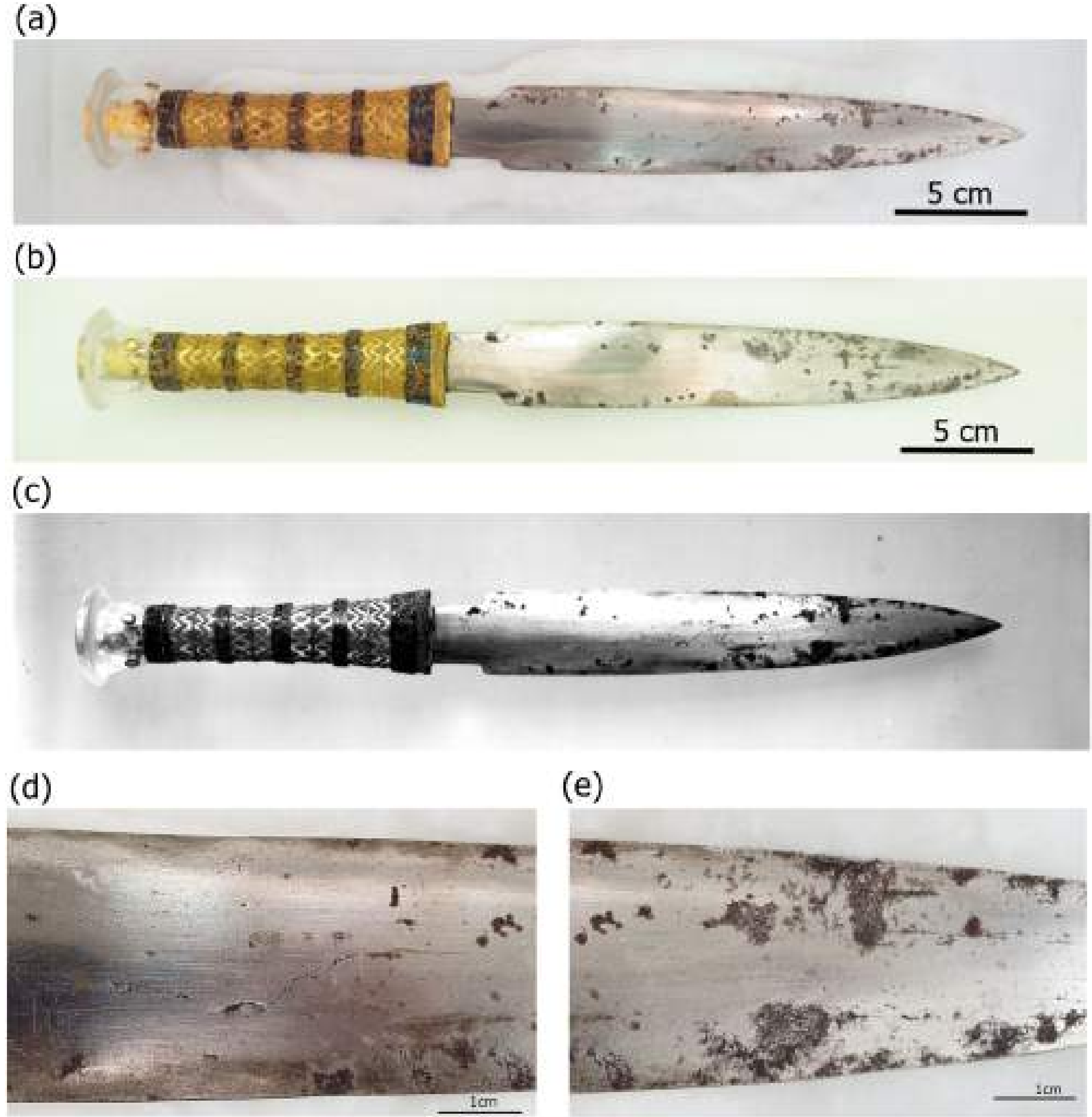

Fig. 1. a, b) Photographs of Tutankhamen's dagger that we took at the Egyptian Museum of Cairo on February 9, 2020. a) One side of the dagger and (b) the other side. It consists of a double-edged metallic iron blade and a hilt made primarily of gold. The length of the dagger is ~35.2 cm (~21.8 cm for the blade and ~13.4 cm for the hilt) and that of the sheath is ~22.5 cm. The thickness of the blade decreases across its width from the center (~2 mm) toward the edges (<1 mm). c) Photograph of Tutankhamen's dagger at the time of the 1925 discovery. This photograph was taken by Harry Burton. Reproduced with permission of the Griffith Institute, University of Oxford. This picture shows the same side as (a) of the 2020 image. d) Photograph of an enlarged portion for one side (a) of the blade with a prominent crack. Fine scratches are oriented along the length of the blade with some oriented across the width of the blade. Note that there is a lack of further corrosion of the blade after the discovery in 1925, comparing the 2020 image (a) with the 1925 image (c). e) Photograph of an enlarged portion for one side (a) of the blade with dark spots.

high-temperature melting and subsequent casting; or low-temperature heating and subsequent forging.

The origin of the Tutankhamen iron dagger is enigmatic, since it is uncertain if the manufacturing technology to make a dagger from meteoric iron was present in the 18th dynasty Egypt. There is written evidence to suggest that Tutankhamen's iron dagger might have been brought from outside Egypt, as mentioned by Comelli et al. (2016). The Amarna letters (or tablets) are diplomatic correspondence, almost all written in Akkadian, an international language at that time. The evidence for iron in the Amarna letters can be found almost exclusively in a list of gifts sent to Amenhotep III (1417–1379 B.C.) of Egypt by Tusratta, the king of Mitanni, which was located southeast Anatolia, when he married the princess Taduhepa to Amenhotep III (Lucas & Harris, 2012; McNutt, 1990; Morkot, 2010; Rainey, 2014). In this document, **habakin(n)u (ha-bal-ki-i-in-nu)** is translated as "iron" (Moran, 1992). According to the translation by W. L. Moran, on VS XII 199 = EA 22 I, 32–35 (p. 51 of Moran, 1992), a dagger is described:

> 1 dagger, the blade of which is of **iron**, its guard, of gold, with designs; its haft of ebony with calf figurines; overlaid with gold; its pommel is of ... -stone; its (...) ..., overlaid with gold, with designs, 6 shekels (= ca. 50 g) gold have been used on it.

A similar description can be found in VS XII 199 = EA 22 III, 7–9 (p. 54 of Moran, 1992):

> 1 dagger, the blade, of **iron**; its guard, of gold, with designs; its hilt, of ...; an inlay of genuine lapis lazuli; its pommel, of hiliba-stone. 5 shekels (= ca. 42 g) gold have been used on it.

Here, we conducted nondestructive chemical analysis of the Tutankhamen iron dagger in February 2020 at the Egyptian Archeological Museum in Cairo, to constrain its manufacturing method and origin.

METHODS

We conducted nondestructive and noncontact chemical analyses of the Tutankhamen meteoritic dagger blade at the Egyptian Museum of Cairo on February 9 and 10, 2020. The optical image of the dagger surface was taken by a 4k high-resolution, high-sensitive camera (α7s, Sony, Japan). A portable scanning X-ray fluorescence (XRF) analytical instrument (ELIO map, XGLab, Italy) was used to measure major and minor elemental abundances of the dagger, the hilt, and the sheath and to survey element distribution on the surface of the metal blade. The analytical head of the ELIO equips a Pd excitation X-ray tube with voltage range of 10–50 kV and current range of 5–200 μA. The excitation X-ray beam is collimated to 1 mm at the sample surface. Fluorescence X-rays, which are emitted from the sample surface, are detected and measured by a 25 mm^2 silicon drift detector. During analyses, the analytical head of the ELIO was mounted on a driving XY stage. Horizontal and vertical positions of analytical points on the sample surface were controlled by a PC, which is connected to the XY stage.

Point analyses were performed with analytical conditions of X-ray tube voltage of 40 kV, tube anode current of 20 μA, working distance of ~1.4 cm, and acquisition time of 60 s. Semiquantitative results were calculated by the fundamental parameter (FP) method. Concentrations of iron (Fe), nickel (Ni), manganese (Mn), and cobalt (Co) were calculated for the metallic areas of the dagger blade. In addition to these elements, concentrations of sulfur (S), chlorine (Cl), calcium (Ca), and zinc (Zn) were calculated for the black (corroded) areas. For the sheath and hilt, concentrations of gold (Au), silver (Ag), copper (Cu), calcium (Ca), and rubidium (Rb) were calculated. Elemental concentrations reported here should be interpreted with caution because these values are semiquantitative data calculated by the FP method. Note that calculations by FP method underestimate Co concentrations in iron-rich materials due to the peak position of Co Kα that overlaps the Fe Kβ peak.

Mapping analyses were conducted with analytical conditions of tube voltage of 40 kV, tube anode current of 100 μA, and working distance of ~1.4 cm. Analyzed areas were scanned by using a step size of 0.9 mm and acquisition time of 1 s per point. Elemental distribution maps of Ni, S, and Cl were obtained by integrating counts in the peak area of each element. Because the degree of detected counts depends on the distance between sample and detector, a curvature of the blade had effects on elemental distribution maps. In order to minimize the effect from the curvature, we made elemental maps of the entire blade by merging small maps obtained individually. In each acquisition of a small map, we adjusted a position of the dagger and a height of the ELIO analytical head to keep distance between the sample surface and the detector constant. Though these efforts reduced effects from curvature of the dagger, we were not able to completely eliminate these effects especially at the edge of the blade. To create color mosaics of elemental distribution maps for the entire surface of the dagger blade, a common color scale for integrating counts in the peak area of each element is used for all the small maps for each scanned area (see Fig. 3). In element distribution maps for selected scanned areas, color scales slightly vary among the maps, depending on integrating counts in the peak area of target elements within the selected scanned area.

For comparison, we conducted nondestructive, noncontact chemical analyses of the Shirahagi iron meteorite, with the same analytical instrument and techniques as stated the above. The Shirahagi iron meteorite is known as a source of a Japanese historical iron sword, Ryuseito (Komatsu et al., 2019), which is stored in the Toyama Science Museum, Toyama, Japan. All the analyses were conducted at the Toyama Science Museum.

RESULTS

The Tutankhamen dagger consists of a double-edged metallic iron blade and a hilt made primarily of gold (Figs. 1a and 1b). The blade shows a roughly polished metallic surface with weak luster and fine scratches (Fig. 1d). A prominent crack of ~5 cm long and ~1 mm wide is present in the central portion of the blade on one side (Fig. 1d). The crack is not linear and is slightly winding. The interior of the crack appears black. Black spots of ~1 mm to ~1 cm wide are present along the edges and in the central area of the blade (Figs. 1a and 1b). Most of the black spots have bumpy, vesiculated surfaces (Fig. 1e). Note that there is a lack of further corrosion of the blade after the discovery in 1925, comparing the 2020 image (Fig. 1a) with the 1925 image (Fig. 1c).

The hilt of the dagger and the associated sheath are made of gold (Fig. 2). The hilt has five bands of ~3 mm to ~1 cm wide, which are decorated with stones such as lapis lazuli, carnelian, and malachite (Arnold et al., 2003). In gold portions between the decorated bands, diamond-shaped and wavy patterns are created with fine gold grains of ~0.5 mm. These stones and gold grains are bonded to the gold surface. The hilt has a pommel of crystal attached to the gold base by several gold pins. The sheath has no accessory materials. The pattern on the sheath is engraved on sheet gold (Fig. 2a).

We conducted semiquantitative analyses of 26 points on the metallic blade, including the black spots and the prominent crack (Table 1). The average Fe, Ni, and Co abundances of the blade are 87.6 ± 0.7 wt%, 11.8 ± 0.5 wt%, and 0.2 ± 0.1 wt%, respectively. The blade contains trace amounts of Mn and Cr, with their concentration below quantitation limit. The black spots show the average Fe content of 79.2 ± 5.6 wt%, varying from 72.8 to 83.8 wt%. The average Ni content is 9.8 ± 1.2 wt%. The sulfur concentration ranges from 0.8 to 5.3 wt% and the Cl content from 3.1 to 10.6 wt%. Trace amounts of Ca, Mn, Zn, and Cr were detected below the quantification limit. The prominent crack shows a similar composition to those of the black spots with 3.1 wt% of S and 3.07 wt% of Cl.

Two points on the gold hilt and the gold sheath were measured, respectively (Figs. 2b and 2c). The flat surface area of the gold hilt was spotted, avoiding the gold grains and stones. The average Au concentrations of the hilt and sheath are 93.2 ± 1.8 wt% and 95.9 ± 0.4 wt%, respectively. Trace amounts of Ag, Cu, and Rb were detected in both hilt and sheath (Table 1). Note that the hilt shows Ca contents of 3.3 and 1.7 wt%, while the sheath contains <0.5 wt% Ca.

Elemental mapping analyses over the whole surface of the blade reveal that Ni, S, and Cl show heterogeneous distributions (Fig. 3). The X-ray maps show a mottled color pattern indicating analogous elemental distribution, including Ni. In some places, discontinuous banded arrangements with cubic symmetry and bandwidth of about 1 mm are observed (Fig. 4).

DISCUSSION

Octahedrite As a Possible Source Iron Meteorite for Tutankhamen's Dagger

The averaged Ni (11.8 ± 0.5 wt%) and Co (0.2 ± 0.1 wt%) contents of the total 13 analyzed points on the metallic iron dagger blade are roughly consistent with those of the two-point analyses (10.8 ± 0.3 wt% Ni and 0.58 ± 0.04 wt% Co) reported by Comelli et al. (2016), confirming the meteoritic origin. Note that the Ni and Co concentrations obtained by the calibration curve method (Comelli et al., 2016) are more accurate than those of our semiquantitative data calculated by the FP method. We may underestimate the Co concentration of the dagger blade because our analyses were not capable of resolving the Co Kα peak from that of the Fe Kβ.

The discontinuous banded arrangements with cubic symmetry and bandwidth of about 1 mm observed in the Ni map of the iron dagger blade suggest the presence of Widmanstätten pattern, where Ni-poor kamacite is exsolved from Ni-rich taenite (Fig. 5). The Widmanstätten pattern on the dagger blade uncovered by Ni mapping is optically unnoticeable due to surface polishing during working. The intermediate Ni content (11.8 ± 0.5 wt%) with the Widmanstätten pattern of about 1 mm thick implies the source meteorite for the Tutankhamen dagger blade to be an octahedrite, which is typically characterized by Ni bands of 0.5–1.3 mm wide and 5–18 wt% of Ni (Scott & Wasson, 1975).

The width of the Ni banded arrangement has some uncertainties. The bandwidth of 1 mm is marginally measurable with the X-ray beam collimated to 1 mm, which tends to generate an excitation volume in the sample ~5 times larger. The orientation of the crystallographic axes of the Ni band relative to the surface of the blade is not known in our nondestructive, noncontact analyses of the iron blade. Such uncertainties considered, classification among fine, medium, or coarse octahedrites is unfeasible on the basis of the observed ~1 mm-thick, Ni bands.

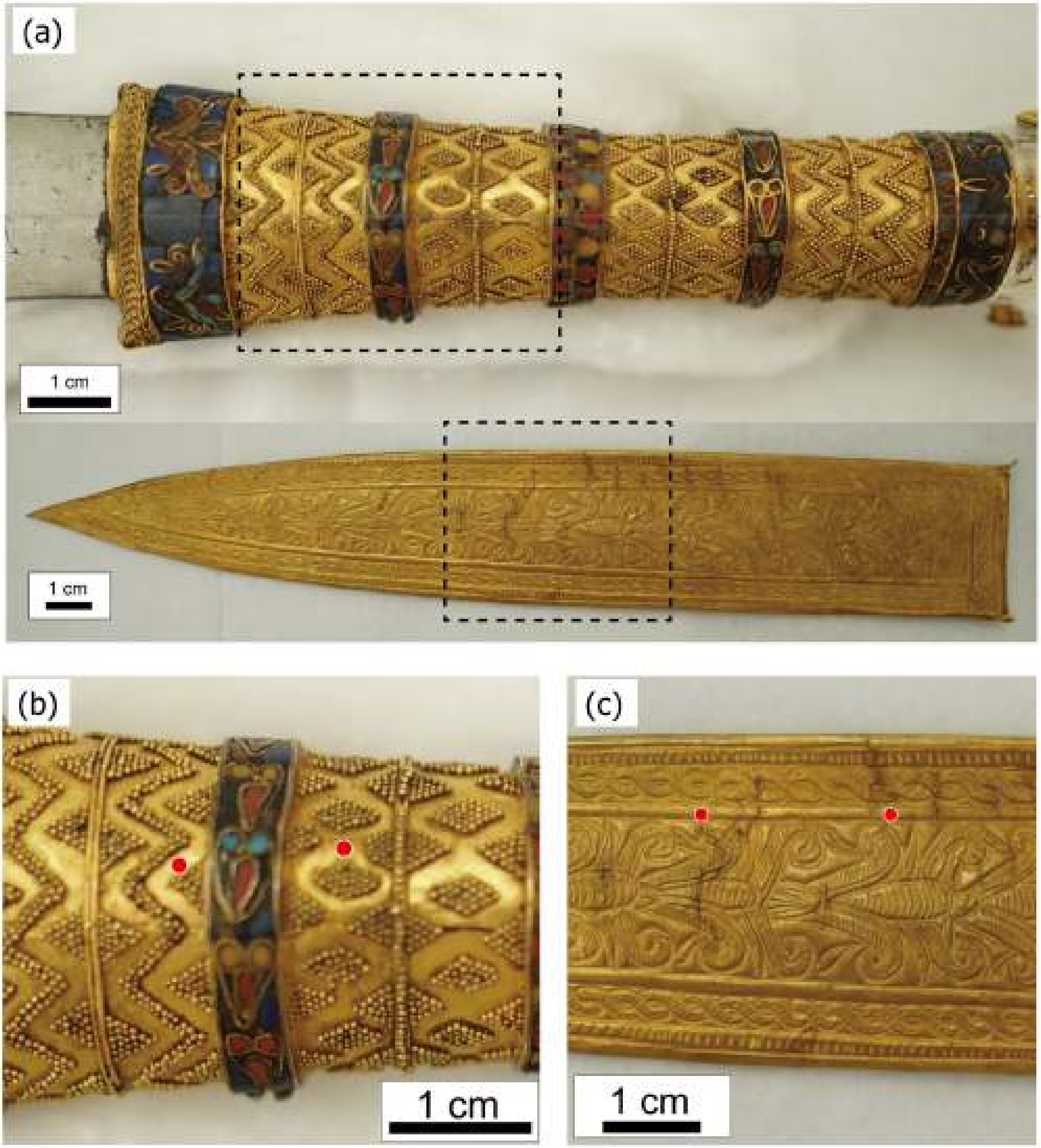

Fig. 2. a) Photograph of the gold hilt of the iron dagger (upper panel) and the associated gold sheath (lower panel). Enlarged images of hatched areas of the gold hilt (b) and the gold sheath (c) of (a). Analytical points of semiquantitative analyses are shown with red circles.

The discontinuous, in-place occurrences of the Ni banded arrangements on the iron dagger blade may be a result either from the partial disruption of the original Widmanstätten pattern due to working, and/or from limited detectability of the nondestructive, noncontact XRF analyses. To demonstrate this possibility, we

Table 1. Averaged semiquantitative results for the blade, hilt, and sheath of the Tutankhamen meteoritic iron dagger.

	Metallic areas (n = 13)		Black areas (n = 13)			Hilt (n = 2)		Sheath (n = 2)	
	wt%	2σ	wt%	2σ		wt%	2σ	wt%	2σ
Fe	87.6	0.7	79.2	5.6	Au	93.2	1.8	95.9	0.4
Ni	11.8	0.5	9.8	1.2	Ag	2.1	0.3	2.6	0.1
Mn	0.4	0.2	0.3	0.2	Ca	2.5	2.3	0.3	0.4
Co	0.2	0.1	0.4	1.0	Cu	1.0	–	0.5	–
S	–	–	3.2	2.5	Rb	0.6	–	0.5	–
Cl	–	–	6.3	4.3					
Ca	–	–	0.6	0.3					
Zn	–	–	0.2	0.1					

obtained Ni elemental map for the Shirahagi iron meteorite (Shima et al., 1981), which is medium octahedrite, with the same analytical instrument and techniques as those used for the analysis of the Tutankhamen dagger blade. We analyzed the Shirahagi sample on site at the Toyama Science Museum (Fig. 6a). The Widmanstätten pattern of about 1mm bandwidth is optically visible on the surface of the Shirahagi sample (Fig. 6b). The Ni map of the Shirahagi sample shows discontinuous banded arrangements with cubic symmetry in places (Fig. 6c). This occurrence of the Widmanstätten pattern in the Ni map is remarkably similar to of that of Tutankhamen's iron dagger (Fig. 5a). This fact shows that common occurrences of discontinuous Ni banded arrangements in places both in the Tutankhamen iron dagger and the Shirahagi iron sample are attributed to technical limitation of nondestructive, noncontact XRF elemental mapping.

Black, Vesicular Spots as Evidence of Heating

The black spots of the blade are chemically distinct from the smooth, metallic areas. The averaged Fe and Ni contents of the black spots are slightly lower than those of the smooth, metallic portions (Table 1). Note that the black spots are more abundant in S and Cl: these have S concentration ranging from 0.8 to 5.3 wt% and Cl concentration ranging from 3.1 to 10.6 wt%, with trace amounts of Mn, Zn, Cr, and Ca. The presence of sulfur indicates that the dark portions originated from troilite, an iron sulfide mineral with the chemical formula FeS. Troilite is a common mineral in iron meteorites and generally occurs as isolated inclusions, mostly rounded nodules enclosed in Fe-Ni metallic areas (e.g., Mittlefehldt et al., 1998). The trace amounts of Mn, Zn, and Cr hint at a minor presence of daubréelite ($FeCr_2S_4$), a mineral commonly coexisting with troilite in iron meteorites (e.g., Mittlefehldt et al., 1998).

The prominent crack of the dagger shows S and Cl abundances similar to those of the black spots, which suggests a common provenance from troilite in the source meteorite. An experimental study of the production of a sword from the Gibeon octahedrite iron meteorite reports the presence of winding cracks with a black interior that originated from troilite inclusions in the source iron meteorite (Taguchi, 1991).

The sulfur contents of the prominent crack in our analysis are much lower than those found in meteoritic troilites, which have about 36 wt% (e.g., Mittlefehldt et al., 1998). The lower sulfur abundance and the variable concentration of 0.8 to 5.3 wt% are probably the result of a loss of sulfur by some heating process under an oxidative environment in the atmosphere, indicated as

$$2FeS + 3/2O_2 = Fe_2O_3 + 2S \text{ (gas)}.$$

The vesicular texture is consistent with loss of sulfur with Fe-oxide formation (e.g., Rietmeijer, 2004).

Evidence of Corrosion in the Black, Vesicular Spots

Chlorine is commonly associated with the ferrous hydroxychloride mineral, akagenéite, β-$Fe_2(OH)_3Cl$, which is a corrosion product of meteorites and ancient iron objects (Buchwald & Koch, 1995; Tilley & Bevan, 1998). Chemical studies of Cl-containing phases in buried iron archaeological artefacts show that the variation in Cl content is associated with the Fe valence state, with low Cl content (about 5 wt%) in the region with Fe(III), and high Cl content (about 15%) with Fe(II) (Réguer et al., 2007). The variable Cl content in the black spots may be attributed to the

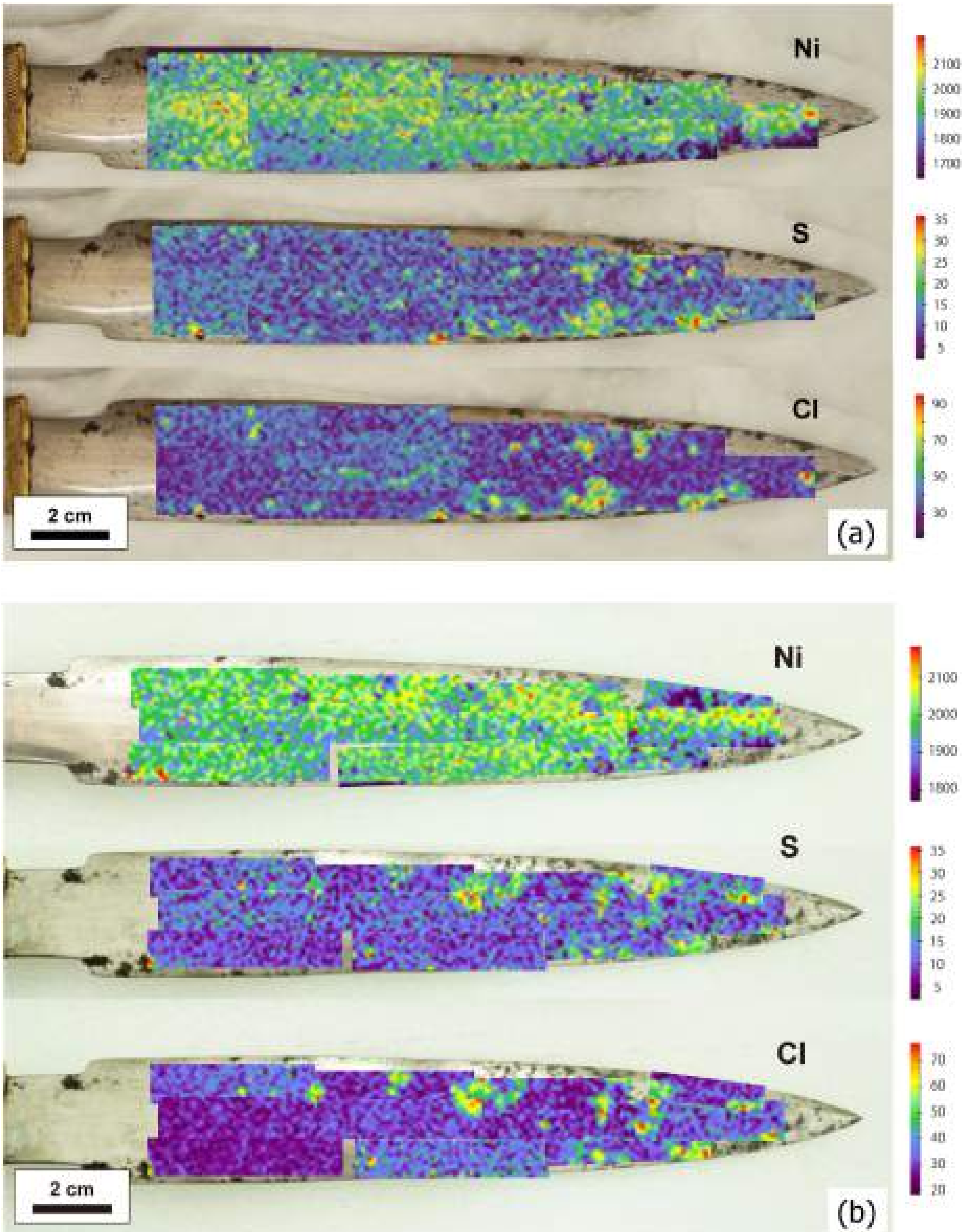

Fig. 3. Ni, S, and Cl elemental distribution maps of both sides of the Tutankhamen iron dagger blade, analyzed by the portable XRF. a) One side of the dagger blade shown in Fig. 1a. b) The other side of the dagger blade shown in Fig. 1b. All the maps show mottled color patterns indicative of analogous elemental distribution. In S and Cl maps, high concentration areas are heteogeneously present. Numbers of color scale bars show integrating counts in the peak area of each element.

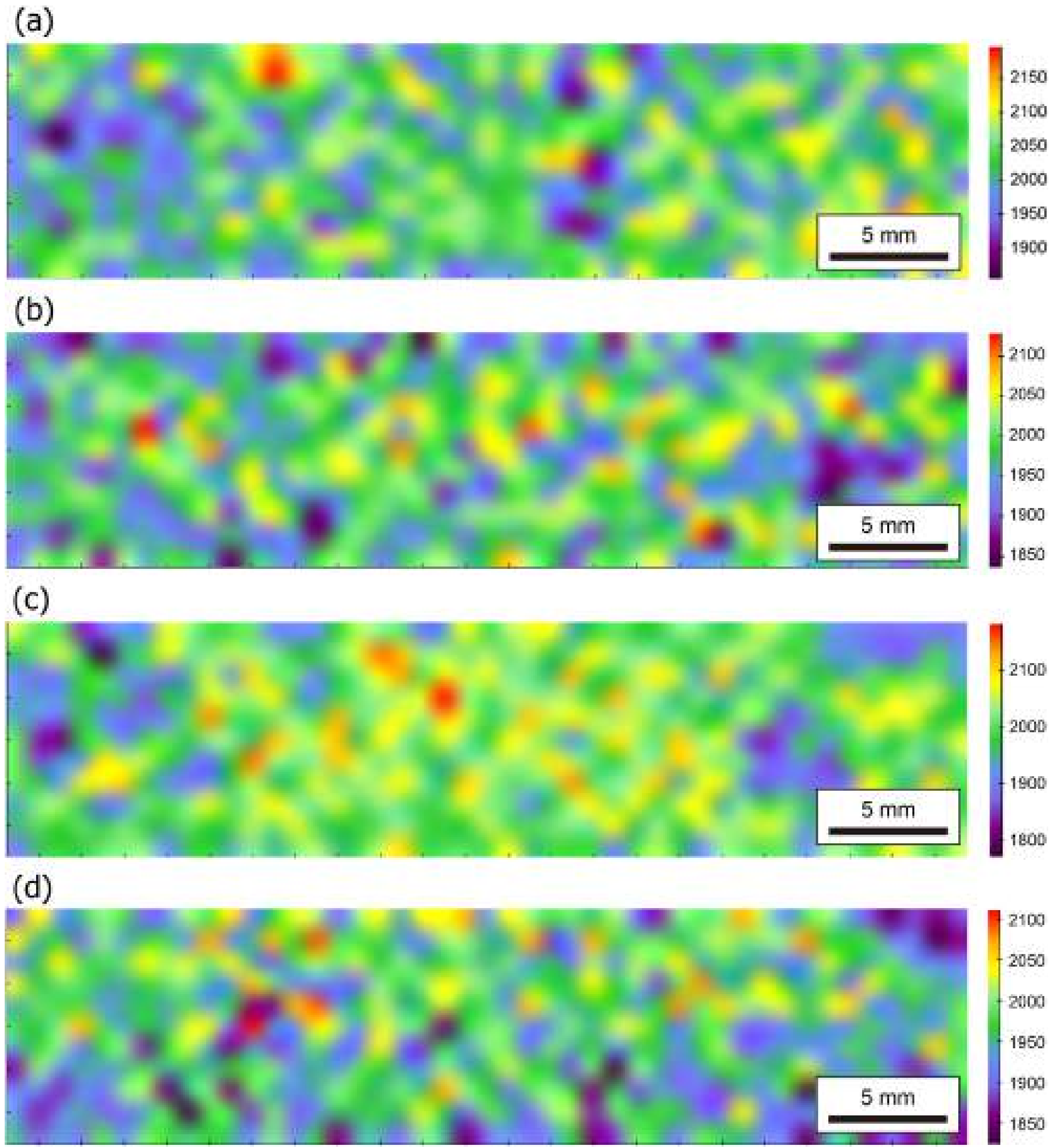

Fig. 4. Ni distribution maps of selected areas of Fig. 3, showing discontinuous banded arrangements in places with "cubic" symmetry and bandwidth of about 1 mm, suggesting the presence of Widmanstätten pattern. a) Upper left area and (b) upper middle area of the one side of the dagger blade (Fig. 3a). c) Middle left area and (d) upper middle of the other side of the dagger blade (Fig. 3b). Numbers of color scale bars show integrating counts in the peak area of Ni within each analyzed area.

inhomogeneous presence of Fe(II) and Fe(III) as a result of oxidation during heating when the dagger blade was manufactured, and subsequent corrosion either before it was buried with the mummy or while it was stored in the Tutankhamen tomb. The photo of the dagger blade upon discovery in 1925 (Fig. 1b)

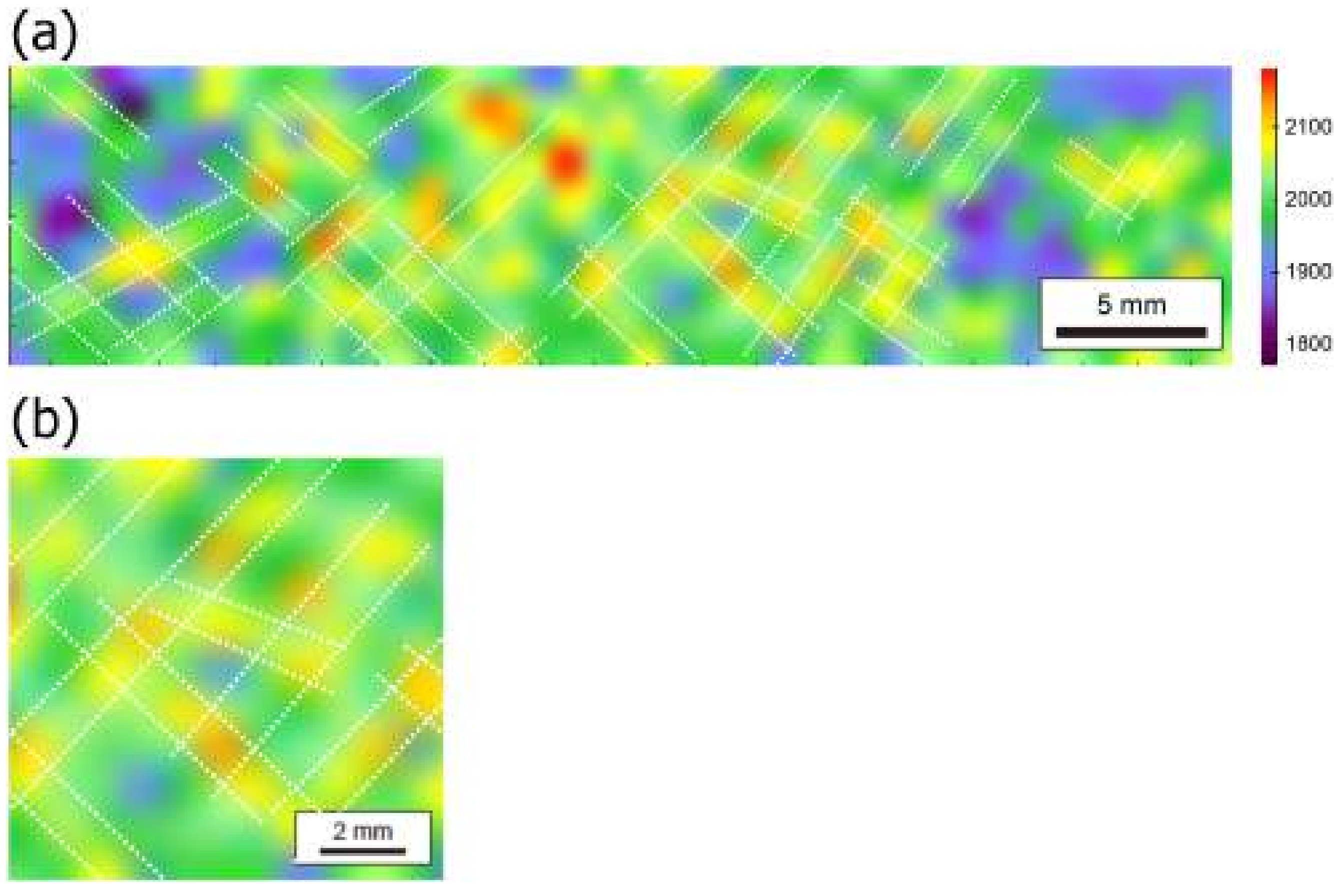

Fig. 5. a) Ni distribution map of Fig. 4b with lines to show discontinuous banded arrangements with cubic symmetry and bandwidth of about 1 mm, suggestive of the Widmanstätten pattern. b) Close-up image of the middle area of (a).

shows the distribution of the black spots, which is almost identical to that of today (Fig. 1a), indicating that the black spots are not the result of corrosion after discovery.

Manufacturing Method of the Tutankhamen Dagger Blade

Our spatially resolved chemical analyses enable us to constrain the manufacturing method of the Tutankhamen iron dagger. First, the preservation of the Widmanstätten pattern of the source medium octahedrite iron meteorite rules out high-temperature melting. Second, the extensive loss of sulfur from the dark, vesicular spots that represent the initial meteoritic troilite inclusions indicates heating around 700 °C or higher, which is consistent with low-temperature heating and forging. An experimental study of forging iron meteorites indicates that iron meteorites with low phosphorous (P) (<0.2 wt%) and low sulfur (S) content (<0.02 wt%) can be easily forged by low-temperature heating at <1100 °C (Taguchi, 1991). In contrast, iron meteorites with higher S (>0.02 wt%) and P contents (>0.2 wt%) are cracked by low-temperature heat forging (Taguchi, 1991). However, the S and P contents of the iron metallic part of Tutankhamen's dagger are both below the detection limit, with <0.1 wt%. Therefore, the low S and P content further supports the conclusion that the manufacturing process was low-temperature heating and forging.

Third, an experimental study of the production of a sword from the Gibeon octahedrite iron meteorite by heating at <1100 °C and forging showed that the sword preserved the original Widmanstätten pattern and that vesicular troilite inclusions in the original Gibeon meteorite resulted in linear black cracks and spots (Taguchi, 1991).

Finally, the presence of the dark, vesicular spots originating from meteoritic troilite inclusions indicates that Fe-Ni metal and the troilite inclusions coexisted without eutectic melting in the heating process of manufacturing the dagger. Since the Fe, Ni-FeS eutectic melting occurs at ~950 °C (Kullerud, 1963), the coexisting Fe-Ni metal and troilite inclusions

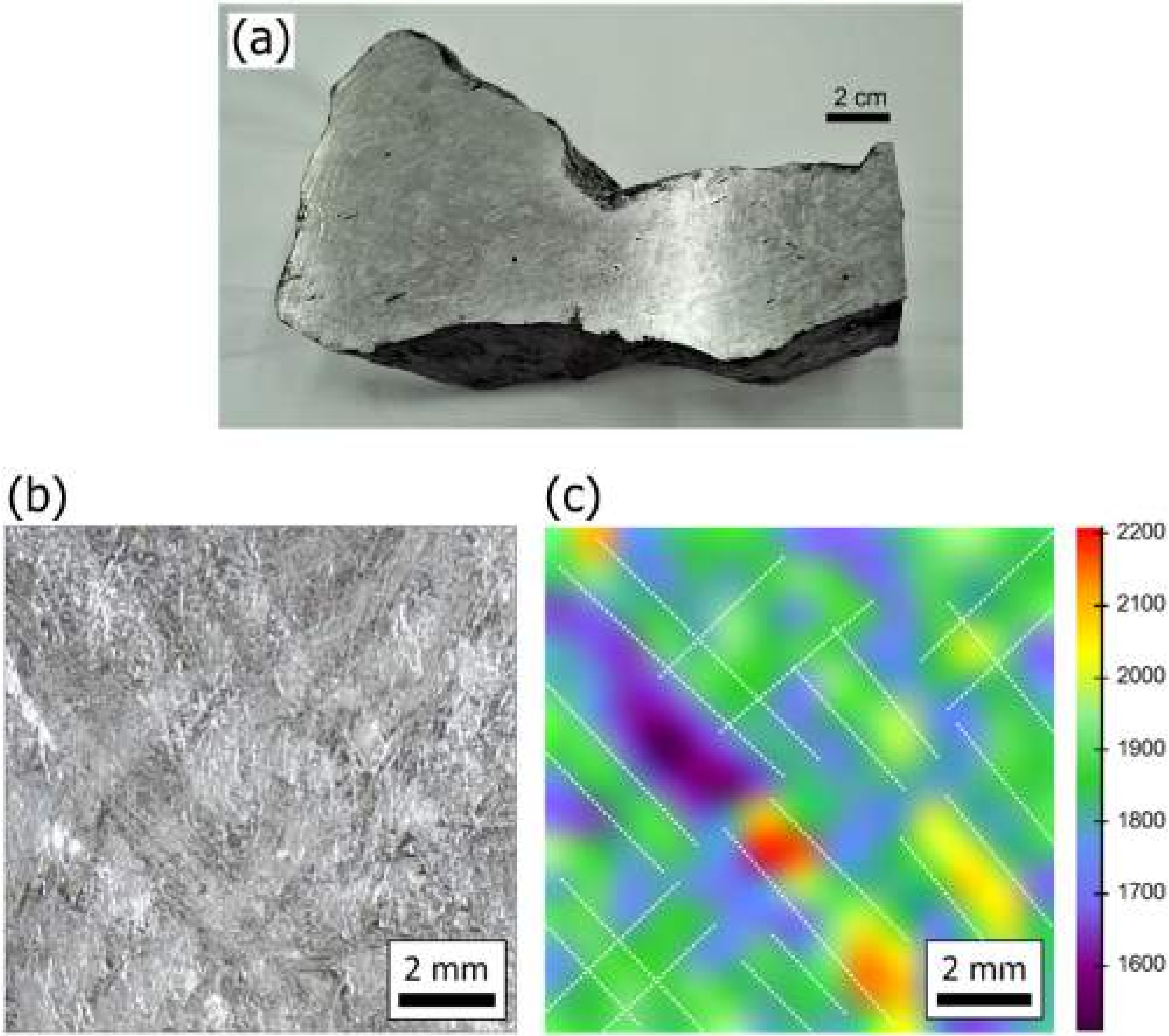

Fig. 6. a) Photograph of the Shirahagi IVA octahedrite sample taken at the Toyama Science Museum. b) Photograph of the close-up view of the surface of the Shirahagi sample of (a). The Widmanstätten pattern is noticeable. c) Ni distribution map for the same surface area of the Shirahagi sample in (b), showing discontinuous banded arrangements with cubic symmetry, indicative of the Widmanstätten pattern.

represented by the dark, vesicular spots indicates that the heating temperature should not have exceeded ~950 °C during the manufacture of Tutankhamen's dagger blade. These lines of evidence lead to a conclusion that the Tutankhamen iron blade was made by low-temperature heat forging at less than 950 °C.

Origin of the Tutankhamen Dagger

While the gold sheath with no decorative materials bonded on the surface has lower Ca content (0.3%), the gold hilt includes a few percent of calcium (Table 1). The average Ca content is greater than the silver content (Table 1) and such high Ca content is somewhat unusual. Lower abundance of Ca (0.1–1.1 wt%) was reported on Tutankhamen's gold mask (Uda et al., 2007). The previous study (Uda et al., 2007) implies that Ca might originate from the glue used for fixing gold powder and thin gold sheet on the surface of the mask. Organic glue can contain calcium carbonate or gypsum as a filler. We suggest that the Ca detected on the gold hilt may be attributed to adhesive substances used for decorating the hilt with the stones and fine gold grains (Fig. 2b).

Adhesive materials used at the time in Egypt were organic glue derived from organic materials and plaster made from either calcium carbonate (lime) or gypsum. Organic glue was commonly used as the adhesive material for fixing gold powders and gold leaf on wood (Hatchfield & Newman, 1991; Rifai & El Hadidi, 2010). It is reported that glue was used in gilded wood samples found at the tomb of Tutankhamen (Rifai & El Hadidi, 2010). We consider that Ca detected on the gold hilt was not derived from an organic glue but from a plaster-type adhesive. This is because an organic glue might be adequate for bonding gold powders and thin gold sheet on porous materials such as wood, but might be inadequate for bonding the larger stones and gold grains onto the nonporous gold hilt. Instead, we suggest that the Ca on the gold hilt originated from either lime plaster or gypsum plaster. The lack of sulfur on the hilt (Table 1) indicates that lime plaster, such as quicklime (CaO) or hydrated lime ($CaOH_2$), were used as the bonding material, instead of burnt plaster from gypsum ($CaSO_4 \cdot 1/2H_2O$).

High temperature (900–950 °C) is necessary for producing quicklime ($CaCO_3 \rightarrow CaO + CO_2$), but production of burnt plaster from natural gypsum ($CaSO_4 \cdot 2H_2O \rightarrow CaSO_4 \cdot 1/2H_2O + 3/2H_2O$) is possible at lower temperature (150 °C). Considering the environmental conditions in Egypt and the lack of wood for fuel, burnt plaster might have been a favorable choice there. However, the adhesive technology using burnt plaster became popular much later in Egypt (Arnold et al., 2003). Furthermore, the use of lime plaster in Egypt started during the Ptolemaic period (305–30 B.C.; Carter & Mace, 1923–1927–1933).

The Amarna letters are diplomatic correspondence from the Egyptian royal archives (Moran, 1992). The letters mention a list of gifts made of iron, including an iron dagger with a gold sheath, that were sent to Amenhotep III (1417–1379 B.C.) of Egypt by Tusratta, the king of Mitanni, when he married the princess Taduhepa to Amenhotep III, who was grandfather of Tutankhamen (Lucas & Harris, 2012; McNutt, 1990; Morkot, 2010; Rainey, 2014). The Amarna letters may be written evidence to suggest that the Tutankhamen's iron dagger might have been brought from outside Egypt, as mentioned by Comelli et al. (2016). Iron processing technology and the use of lime plaster was already prevalent in Mitanni and Hittite regions at that time (Moorey, 1994). The Ca-bearing, sulfur-lacking plaster used on the gold hilt may support the idea that the Tutankhamen meteoritic iron dagger was brought as a gift from Mitanni, as recorded in the Amarna letters.

CONCLUSION

We conducted nondestructive chemical analysis of nicely preserved Tutankhamen's meteoritic iron dagger in February 2020 on site at the Egyptian Archeological Museum in Cairo, in order to constrain its manufacturing method and origin. Elemental mapping of Ni on the blade surface shows discontinuous banded arrangements in places with "cubic" symmetry and bandwidth of about 1 mm, suggesting the Widmanstätten pattern. The intermediate Ni content (11.8 ± 0.5 wt%) with the Widmanstätten pattern implies the source iron meteorite for the Tutankhamen dagger blade to be octahedrite. Sulfur-rich black spots randomly distributed on the blade surface are likely remnants of troilite (FeS) inclusions in the source iron meteorite. The preserved Widmanstätten pattern and the remnant troilite inclusion show that the iron dagger was manufactured by low-temperature (<950 °C) heat forging. The gold hilt with a few percent of calcium lacking sulfur suggests the use of lime plaster instead of gypsum plaster as an adhesive material for decorations on the hilt. Since the use of lime plaster in Egypt started during the Ptolemaic period (305–30 B.C.), the Ca-bearing gold hilt hints its foreign origin, possibly from Mitanni, Anatolia, as suggested by one of the Amarna letters saying that an iron dagger with gold hilt was gifted from the king of Mitanni to Amenhotep III, the grandfather of Tutankhamen.

Acknowledgments—We are grateful to Mr. Masaki Noke, ambassador of Japan to the Arab Republic of Egypt, for arranging permission from the Egyptian government for us to analyze Tutankhamen's iron dagger. We also express our sincere thanks to Dr. Sabah Abdel Razek, director of the Egyptian Museum, for her kind hospitality during the measurements at the museum, and to Dr. Akiko Nishizaka of the Japan International Cooperation Center (JICE) in Cairo for providing us the information on the reference about adhesive materials used for Tutankhamen's mask. We also thank the local staff of the Japan International Cooperation Agency (JICA) Egypt Office for their support throughout this project. We thank the Toyama Science Museum to provide us with an opportunity to conduct nondestructive XRF analyses of the Shirahagi iron meteorite and the Ryuseito. We are grateful to C. Corrigan and the anonymous reviewer for careful reviews, which substantially improved this paper.

Data Availability Statement—The data that support the findings of this study are available from the corresponding author upon reasonable request.

Editorial Handling—Dr. Kevin Righter

REFERENCES

Arnold, D., Strudwick, H. M., and Strudwick, N. 2003. *The Encyclopedia of Ancient Egyptian Architecture*, 101–33. Princeton, New Jersey: Princeton University Press.

Bjorkman, J. K. 1973. Meteors and Meteorites in the Ancient Near East. *Meteoritics & Planetary Science* 8: 91–132.

Buchwald, V. F., and Koch, C. B. 1995. Hibbingite (Beta-$Fe_2(OH)_3Cl$), a Chlorine-Rich Corrosion Product in Meteorites and Ancient Iron Objects. *Meteoritics* 30: 493.

Carter, H., and Mace, A. C. 1923–1927–1933. *The Tomb of Tut*Ankh*amen*. London: Cassell and Company Ltd.

Comelli, D., D'Orazio, M., Folco, L., El-Halwagy, M., Frizzi, T., Alberti, R., Capogrosso, V. et al. 2016. The Meteoritic Origin of Tutankhamun's Iron Dagger Blade. *Meteoritics & Planetary Science* 51: 1301–9.

Hatchfield, P., and Newman, R. 1991. Ancient Egyptian Gilding Methods. In *Gilded Wood: Conservation and History*, edited by D. Bigelow, 27–47. Madison, Connecticut: Sound View Press.

Johnson, D., Tyldesley, J., Lowe, T., Withers, P. J., and Grady, M. M. 2013. Analysis of a Prehistoric Egyptian Iron Bead with Implications for the Use and Perception of Meteorite Iron in Ancient Egypt. *Meteoritics & Planetary Science* 48: 997–1006.

Komatsu, M., Yamaguchi, A., Ito, M., Yoneda, S., Saito, T., Ohgane, T., Hayashi, T., Sakamoto, M., Mikouchi, T., and Kimura, M. 2019. Ryuseito: The Japanese Swords Made from Shirahagi Iron Meteorite (Abstract #6216). 82nd Annual Meeting of The Meteoritical Society. LPI Contribution No. 2157.

Kullerud, G. 1963. The Fe-Ni-S System. *Carnegie Institute of Washington Yearbook* 62: 175–89.

Lucas, A., and Harris, J. 2012. *Ancient Egyptian Materials and Industries*. Mineola, New York: Dover Publications Inc.

McNutt, P. M. 1990. *The Forging of Israel: Iron Technology, Symbolism and Tradition in Ancient Society*. Sheffield, UK: Sheffield Academic Press.

Mittlefehldt, D. W., McCoy, T. J., Goodrich, C. A., and Kracher, A. 1998. Non-Chondritic Meteorites from Asteroidal Bodies. In *Planetary Materials*, Reviews in Mineralogy Vol. 36, edited by Papike, J. J., 4.1–4.195. Washington, D.C.: Mineralogical Society of America.

Moorey, P. R. S. 1994. *Ancient Mesopotamian Materials and Industries: The Archaeological Evidence*. Oxford: Oxford University Press.

Moran, W. L., ed. 1992. *The Amarna Letters*. Baltimore, Maryland: Johns Hopkins University Press.

Morkot, R. 2010. *The A to Z of Ancient Egyptian Warfare*. Lanham, Maryland: Scarecrow Press.

Nakai, I., Abe, Y., Tantrakarn, K., Omura, S., and Erkut, S. 2008. Preliminary Report on the Analysis of an Early Bronze Age Iron Dagger Excavated from Alacahöyük. *Anatolian Archaeological Studies/Kaman-Kalehöyük* 17: 321–3.

Rainey, A. F. 2014. *The El-Amarna Correspondence*. Leiden: Brill Academic Publishers.

Réguer, S., Dillmann, P., and Mirambet, F. 2007. Buried Iron Archaeological Artefacts: Corrosion Mechanisms Related to the Presence of Cl-Containing Phases. *Corrosion Science* 49: 2726–44.

Rietmeijer, F. J. M. 2004. Dynamic Pyrometamorphism During Atmospheric Entry of Large (~10 Micron) Pyrrhotite Fragments from Cluster IDPs. *Meteoritics & Planetary Science* 39: 1869–87.

Rifai, M. M., and El Hadidi, N. M. N. 2010. Investigation and Analysis of Three Gilded Wood Samples from the Tomb of Tutankhamen. In *Decorated Surfaces on Ancient Egyptian Objects: Technology, Deterioration and Conservation*, edited by J. Dawson, C. Rozeik, and M. Wright, 16–24. London: Archetype Publications.

Scott, E. R. D., and Wasson, J. T. 1975. Classification and Properties of Iron Meteorites. *Reviews of Geophysics and Space Physics* 13: 527–46.

Shima, M., Yabuki, S., Kimura, T., and Yabuki, H. 1981. *Bulletin of the National Science Museum Series* E4: 19.

Stevenson, A. E. 2009. *The Predynastic Egyptian Cemetery of el-Gerzeh. Social Identities and Mortuary Practices*. Leuven: Peeters Publishers.

Taguchi, I. 1991. Natural Scientific Research of Meteoritic Iron (Written in Japanese). *Bulletin of the National Museum of Japanese History* 35: 355–72.

Tilley, D. B., and Bevan, A. W. R. 1998. The Prolonged Weathering of Iron and Stony-Iron Meteorite and Their Anomalous Contribution to the Australian Regolith. In *New Approaches to an Old Continent, Proceedings of the 3rd Australian Regolith Conference, Kalgoorlie, Western Australia*, edited by G. Taylor and C. F. Pain, 77–88. Perth: Cooperative Research Centre for Landscape Evolution & Mineral Exploration (CRC LEME).

Uda, M., Yoshimura, S., Ishizaki, A., Yamashita, D., and Sakuraba, Y. 2007. Tutankhamen's Golden Mask Investigated with XRDF. *International Journal of PIXE* 17: 65–76.